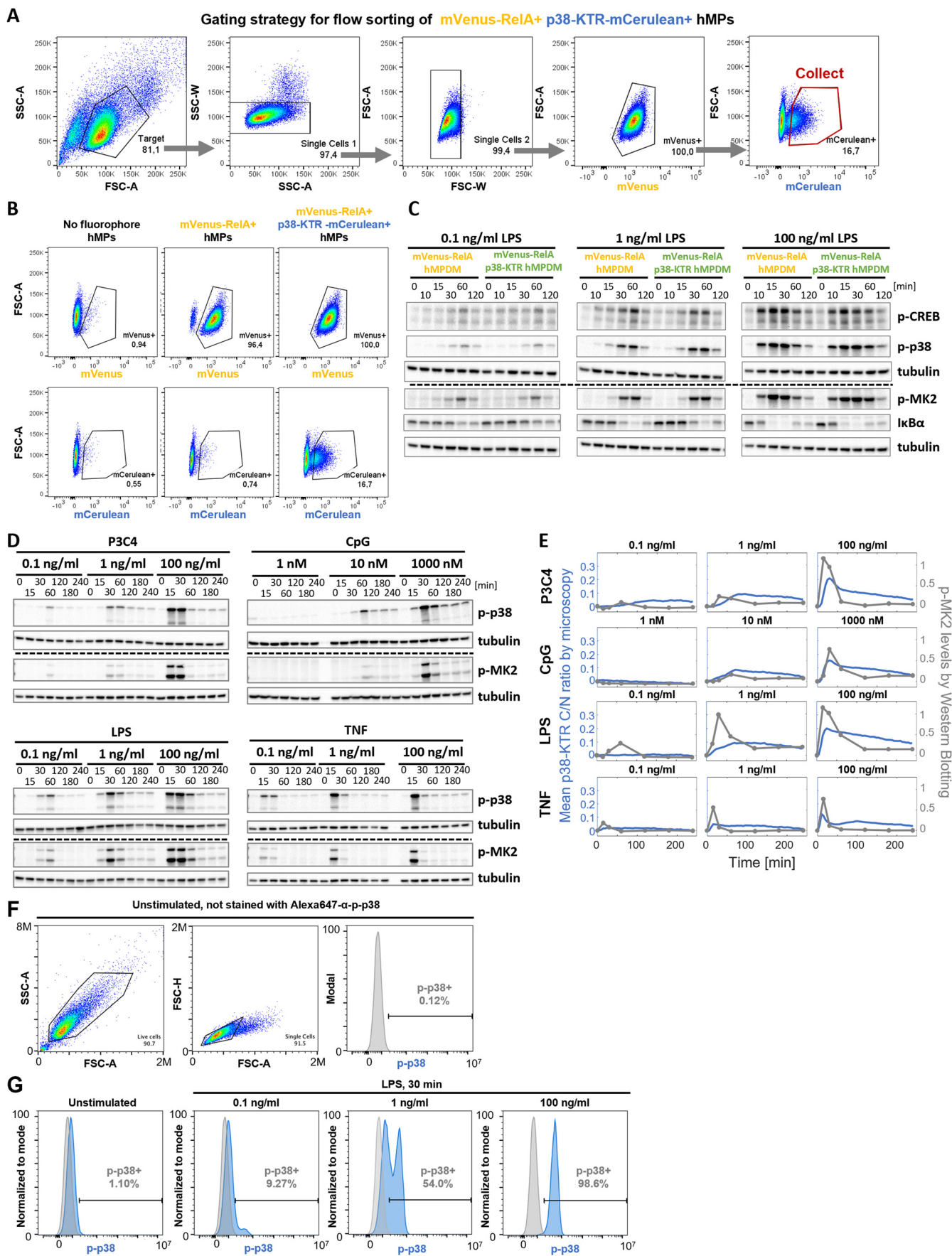
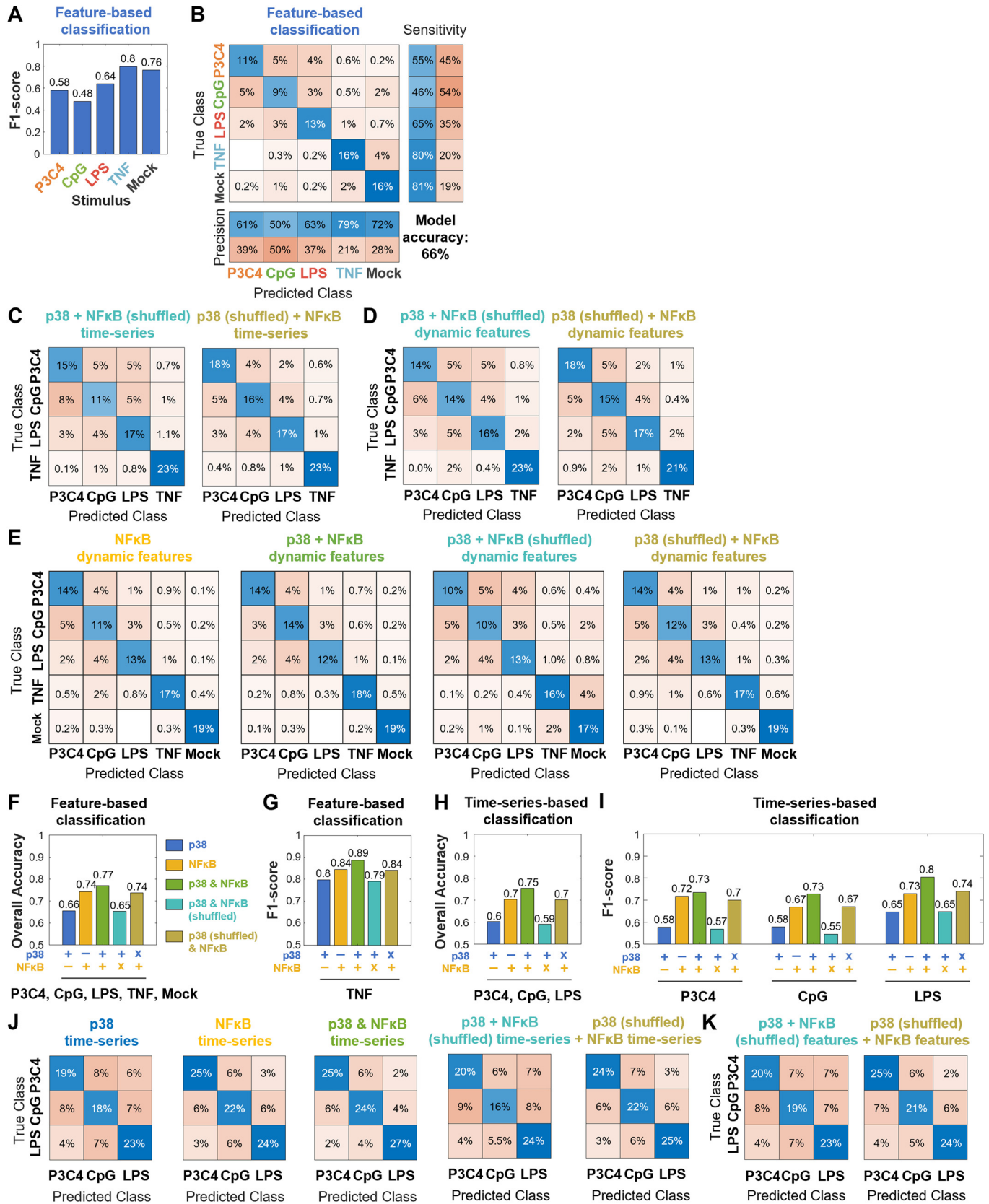


Expanded View Figures

Figure EV1. Quality control of the experimental system for quantifying p38 and NF κ B activity dynamics in murine macrophages.

(A) Gating strategy for FACS of mVenus-RelA⁺ p38-KTR-mCerulean⁺ hMPs. (B) mCerulean and mVenus expression by flow cytometry in WT hMPs, mVenus-Rela hMPs, and mVenus-Rela hMPs transduced with p38-KTR-mCerulean before FACS. (C) Signaling responses to three LPS doses over 2 h in mVenus-Rela p38-KTR-mCerulean hMPDs compared to parent cell line by Western Blotting for phospho-p38, phospho -MK2, phospho-CREB, and I κ B α protein levels. Quantification in Fig. 1B. (D) Bulk p-p38 and p-MK2 protein levels in hMPDs measured by Western Blotting in response to indicated stimulations over 4 h. Quantification in Figs. 1E and EV1D. (E) Comparison of p38 activity over 4 h in hMPDs measured by p38-KTR microscopy (mean of trajectories) and by bulk phospho-MK2 levels measured by Western Blotting in response to three doses of P3C4, CpG, LPS, or TNF (0.1, 1, 100 ng/ml for P3C4, LPS, TNF; 1, 10, 1000 nM for CpG). Western Blotting quantification: band intensities were background corrected, normalized to tubulin control, normalized across multiple membranes using an internal control sample, and baseline-deducted; depicting data from a single experiment (Western Blot membrane shown in Fig. EV1E). For microscopy, the mean of means of trajectories from two biological replicates is shown (in total: 923, 1171, 970, and 1055 cells included in the analysis for P3C4, CpG, LPS, and TNF, respectively; same data as in Fig. 1E). (F) Gating strategy for flow cytometry measurements of intracellular p-p38 levels in hMPDs. (G) Example quantification of p-p38⁺ fraction of cells stimulated with indicated doses of LPS for 30 min (blue). The fluorescence signal of an unstimulated, unstained sample is used to define a cutoff between p-p38⁺ and p-p38⁻ cells (gray). Data from one experiment are displayed.





◀ **Figure EV2. Machine learning classifications of p38 and NFκB activities in response to four high-dose ligand stimulations or PAMP stimulations using shuffled activities as negative controls.**

(A, B) F1 scores by class and confusion matrix of decision tree ensemble classification of p38 dynamic features in response to mock and high-dose P3C4, CpG, LPS, and TNF stimulations. Data from two pooled biological replicates are used. (C, D) Confusion matrices of machine learning classification of NFκB ("shuffled": incorrectly matched NFκB activities from cells randomly selected from all classes) + p38 (left) or NFκB + p38 ("shuffled": incorrectly matched p38 activities from cells randomly selected from all classes) (right) time-series (C) or dynamic features (D) in response to high-dose P3C4, CpG, LPS, and TNF stimulations. Data from two pooled biological replicates are used. (E) Confusion matrices of machine learning classification of decision tree ensemble classification of NFκB only, NFκB + p38, NFκB ("shuffled": incorrectly matched NFκB activities from cells randomly selected from all classes) + p38, or NFκB + p38 ("shuffled": incorrectly matched p38 activities from cells randomly selected from all classes) dynamic features in response to mock and high-dose P3C4, CpG, LPS, and TNF stimulations. Data from two pooled biological replicates are used. (F, G) Overall classification accuracy (F) and F1 score for TNF class (G) in machine learning classifications using p38 only, NFκB only, NFκB + p38, NFκB ("shuffled": incorrectly matched NFκB activities from cells randomly selected from all classes) + p38, NFκB + p38 ("shuffled": incorrectly matched p38 activities from cells randomly selected from all classes) dynamic features in response to mock and high-dose P3C4, CpG, LPS, and TNF stimulations. Data from two pooled biological replicates are used. (H-J) Overall classification accuracy (H), F1 scores for individual classes (I), and confusion matrices (J) for machine learning classifications of time series using p38 only, NFκB only, NFκB + p38, NFκB ("shuffled": incorrectly matched NFκB activities from cells randomly selected from all classes) + p38, or NFκB + p38 ("shuffled": incorrectly matched p38 activities from cells randomly selected from all classes) in response to high-dose P3C4, CpG, and LPS stimulations. Data from two pooled biological replicates are used. (K) Confusion matrices of machine learning classification of NFκB (shuffled among all cells in all classes) + p38 (left) or NFκB + p38 (shuffled among all cells in all classes) (right) dynamic features in response to high-dose P3C4, CpG, and LPS stimulations. Data from two pooled biological replicates are used.

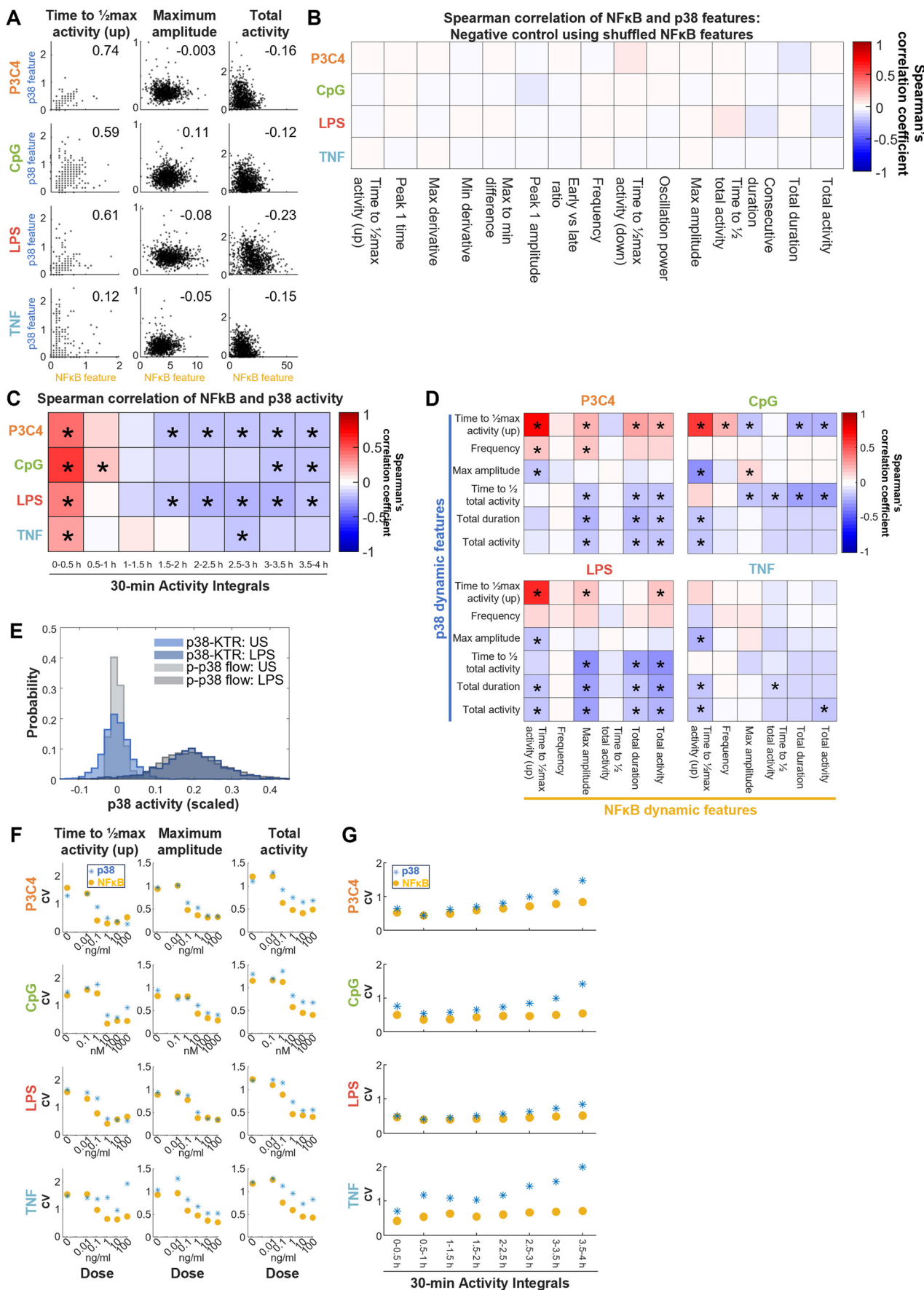
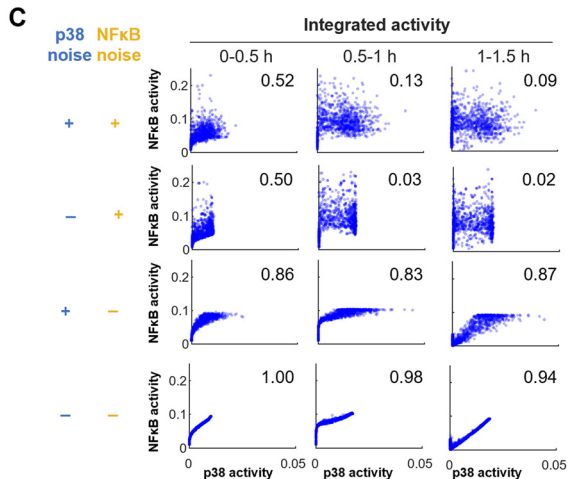
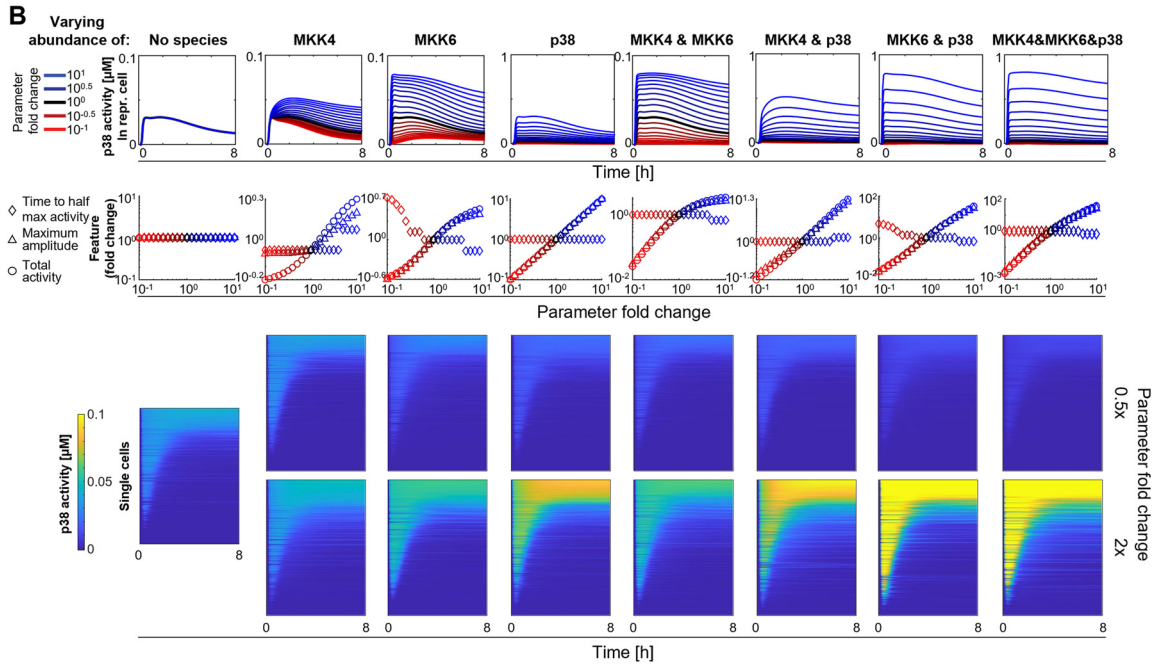
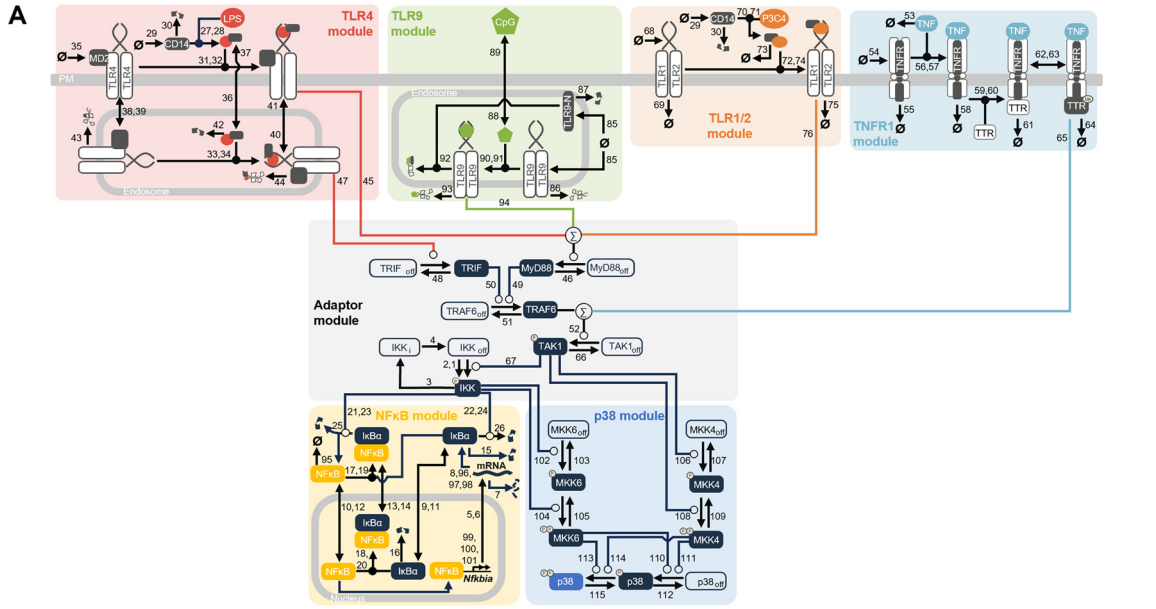


Figure EV3. MAPK p38 and NFκB dynamic features are poorly correlated.

(A) Scatter plots of correlations of selected p38 vs. NFκB dynamic features (as in Fig. 5A) upon stimulation with high-dose P3C4, CpG, LPS, or TNF. Number indicates the Spearman correlation coefficient. Data from two pooled biological replicates are depicted. (B) Negative control: Spearman correlation coefficients (CCs) between indicated p38 dynamic features and corresponding NFκB dynamic feature using NFκB features randomly shuffled with respect to p38 features among cells within a stimulation condition for stimulation with high-dose P3C4, CpG, LPS, or TNF. The asterisk indicates a statistically significant correlation ($p < 0.05$) with $|CC| > 0.15$. Data from two pooled biological replicates are used. (C) Spearman correlation coefficients (CC) between integrals of p38 activity over 30 min from 0 to 4 h and corresponding NFκB integrals upon stimulation with high-dose P3C4, CpG, LPS, or TNF. The asterisk indicates a statistically significant correlation ($p < 0.05$) with $|CC| > 0.15$. Data from two pooled biological replicates are used. (D) Spearman correlation coefficients (CCs) between indicated p38 dynamic features and all indicated NFκB dynamic features upon stimulation with high-dose P3C4, CpG, LPS, or TNF. The asterisk indicates a statistically significant correlation ($p < 0.05$) with $|CC| > 0.15$. Data from two pooled biological replicates are used. (E) Comparison of heterogeneity of p38 activity measured by flow cytometry (gray) and p38-KTR microscopy (blue) in unstimulated cells and upon 30 min 100 ng/ml LPS stimulation. For each assay, the mean of the unstimulated sample is deducted from each distribution. The flow cytometry distributions are scaled using the distance between the peaks of lognormal fits to the unstimulated and the stimulated distributions. Microscopy: Data from two pooled biological replicates are used. Flow cytometry: Data from a single experiment are displayed. (F) Coefficient of variation of indicated p38 and NFκB dynamic features upon stimulation across dose range of P3C4, CpG, LPS, or TNF. Data from two pooled biological replicates are used. (G) Coefficient of variation of 30-min p38 and NFκB activity integrals upon stimulation with high-dose P3C4, CpG, LPS, or TNF. Data from two pooled biological replicates are used.



◀ Figure EV4. An integrated mathematical model of MAPK p38 and NFκB activation suggests sources of heterogeneity.

(A) Detailed schematic of mathematical model structure including reaction numbers (see also Dataset EV1). A model of p38 activation via IKK/Tp12/MKK3/6 and TAK1/MKK4 (blue background) is integrated with established models of NFκB activation (yellow) downstream of TLR1/2 (orange), TLR9 (green), TLR4 (red), and TNF receptor (light blue) signaling (Adelaja et al, 2021; Luecke et al, 2023). (B) Parameter sensitivity analysis probes the effect of kinase abundances within the p38 module. Effect of variations of the abundance of indicated kinase(s) on p38 activity of a representative cell (top), p38 dynamic features in a representative cell (middle), and heterogeneous p38 activity trajectories in single cells upon simulated LPS stimulation (bottom). (C) Scatter plots of p38 vs. NFκB integrated activity over indicated 30 min intervals in simulated LPS stimulation with or without simulated molecular noise (i.e., using parameter distributions or fixed parameter values) in p38 and NFκB modules.

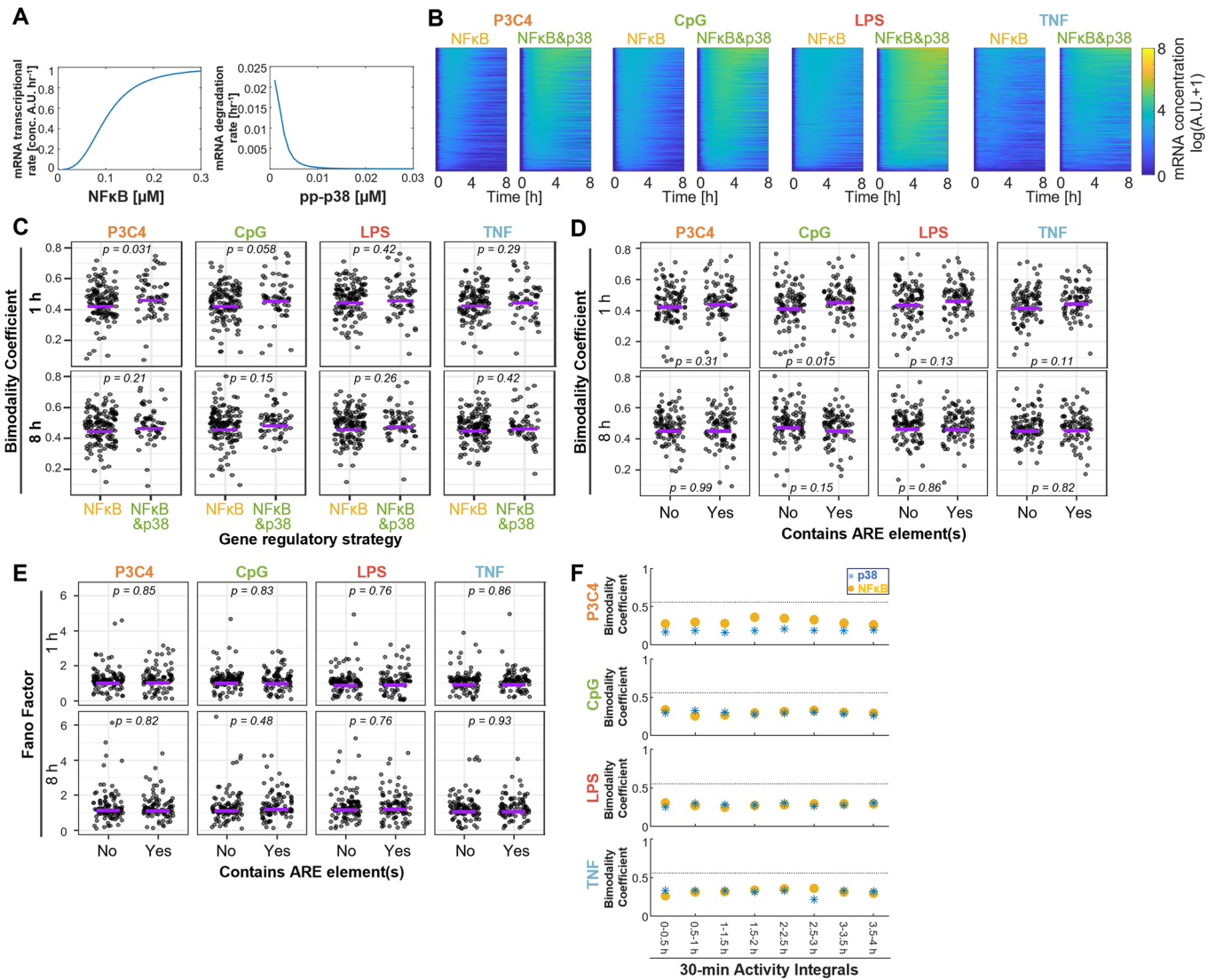


Figure EV5. MAPK p38 signaling contributes heterogeneity to macrophage gene expression responses.

(A) Effect of NFkB and p38 activity levels on simulated mRNA transcription and mRNA-degradation, respectively. (B) Simulated mRNA expression under control of NFkB only or NFkB&p38 over 8 h using experimentally determined NFkB and p38 activity upon high-dose P3C4, CpG, LPS, and TNF stimulation as input to the mathematical model. (C) Bimodality coefficient of all immune response genes regulated by NFkB-only (132 genes) or NFkB&p38 (59 genes) in single cells upon stimulation with P3C4, CpG, LPS, or TNF at 1 and 8 h. Purple line indicates mean. Statistical significance was determined using a permutation test for difference in means using 10000 permutations. Data from one experiment are depicted. (D, E) Bimodality coefficient (D) and Fano Factor (E) of all immune response genes in single cells categorized by absence or presence of ARE-element(s) upon stimulation with P3C4, CpG, LPS, or TNF at 1 and 8 h. Purple line indicates mean. Statistical significance was determined using a permutation test for difference in means using 10000 permutations. Data from one experiment are depicted. (F) Bimodality Coefficients of 30-min p38 and NFkB activity integrals upon stimulation with high-dose P3C4, CpG, LPS, or TNF determined by dual reporter macrophage imaging. Data from two pooled biological replicates are used.